Influence of modified Kevlar nanofibers on the properties of ethylene-propylene-diene monomer rubber

Zhang Yangyang, Zhao Dongwei, Zhao Xin, Dai Yize, Lan Bo, Zuo Yan, Jia Hongbing*

(Key Laboratory of Soft Chemistry and Functional Materials, Ministry of Education, Nanjing University of Science and Technology, Nanjing 210094, Jiangsu, China)

Abstract: With the development of hypersonic weapons, their harsh thermal environment making it crucial to enhance the comprehensive performance of thermal protection materials. In this paper, Kevlar nanofibers (KNFs) were coated with nano-silica through in-situ growth on their surface to obtain KNFs@SiO_2. The influence of γ-aminopropyltriethoxysilane (KH550) modified KNFs@SiO_2 on the ablation resistance and mechanical properties of ethylene propylene diene monomer (EPDM) was investigated. The results showed that compared to EPDM, the tensile strength and elongation at break of the KNFs@SiO_2/EPDM composite filled with 5 parts of KH550 modified KNFs@SiO_2 (KKNFs@SiO_2) increased by 235.5% and 65.4%, respectively, while the linear ablation rate and mass ablation rate decreased by 69.9% and 47.6%, respectively.

Key words: KKNFs@SiO_2; ethylene-propylene-diene monomer rubber; mechanical properties; ablation resistance

Classification number: TQ333.4 **Article number:** 1009-797X(2026)03-0044-08

Document code: B **DOI:**10.13520/j.cnki.rpte.2026.03.011

In recent years, with the development of hypersonic weapons, the thermal environment they face has become increasingly severe, and the requirements for the ablation resistance and mechanical properties of insulation materials have also been rising. However, the ablation resistance and mechanical properties of traditional insulation layer materials have reached their limits, making it difficult to meet the more stringent thermal protection requirements of power systems. Ethylene propylene diene monomer (EPDM), as a new type of flexible ablation-resistant material, has attracted considerable attention in recent years. It has low density, good thermal-oxidative aging resistance, and high thermal decomposition temperature, but it also has problems such as poor mechanical properties, weak charring ability, and low polarity. Various fibrous fillers and resin fillers are often used to compensate for the defects of EPDM. Zhang Chonggeng et al. reinforced EPDM with zinc borate, solid chlorinated paraffin, and ablation-resistant boron resin. The results showed that when the amounts of zinc borate, solid chlorinated paraffin, and ablation-resistant boron resin were 9, 30, and 10 parts, respectively, compared to the index values, the mass ablation rate and linear ablation rate of the composite material decreased by 13.3% and 19.0%, respectively, and the tensile strength and elongation at break increased by 24.5% and 75.6%, respectively. However, the density was significantly higher than the index value. Overall, although this method can enhance the mechanical properties and ablation resistance of the composite material to some extent, it results in a higher density of the composite material.

Nanomaterials, with their unique small-size effect and quantum tunneling effect, have experienced rapid development in recent years. Kevlar fibers exhibit high

---

Biography: Zhang Yangyang (2003-), male, is an undergraduate student currently pursuing his studies, primarily focusing on research in polymer materials.

strength (9250~11100 MPa), high modulus (over 200 GPa), and low density (1.57 g/cm^3). By undergoing deprotonation, Kevlar fibers can be nano-dispersed into Kevlar nanofibers (KNFs), combining the advantages of Kevlar fibers, such as high strength, high modulus, and low density, with the nano-effects of high-performance polymer nanofibers, including high specific surface area and high aspect ratio. After further modification, the interfacial interaction between KNFs and EPDM can be significantly enhanced. Wang et al. prepared modified KNFs with good water dispersibility by grafting epoxy groups onto KNFs, and then prepared modified KNFs/XNBR nanocomposites. The results showed that after adding 5 parts of modified KNFs, the tensile strength of the XNBR nanocomposites increased by 182.0%, the tear strength increased by 101.0%, and the mechanical properties were significantly improved.

In this paper, EPDM served as the matrix, and nano-silica was grown in situ on the surface of KNFs. Subsequently, γ-aminopropyl triethoxysilane (KH550) was grafted onto the KNFs through condensation polymerization, resulting in γ-aminopropyl triethoxysilane (KH550) modified KNFs$^@$SiO$_2$(KKNFs$^@$SiO$_2$). The influence of the amount of KKNFs$^@$SiO$_2$ on the mechanical properties, crosslinking density, thermal stability, and ablation performance of KKNFs$^@$SiO$_2$/EPDM composites was investigated.

1 Experimental part

1.1 Experimental raw materials

Ethylene-propylene-diene monomer (EPDM, 4045; ethylene content, 47.0%; ENB content, 5.0%) was provided by China Petroleum & Chemical Corporation; Kevlar 49 yarn was purchased from DuPont; zinc oxide (ZnO) was provided by Shanghai Jinghua Chemical Reagent Co., Ltd.; stearic acid (StA) was provided by Sinopharm Chemical Reagent Co., Ltd.; dicumyl peroxide (DCP) was provided by AkzoNobel Chemicals Co., Ltd.; zinc borate (ZB) was provided by Qingdao Yusuo Chemical Technology Co., Ltd.; benzoxazine (BA, BZ7413) was provided by Puyang Enying Polymer Materials Co., Ltd.; γ-aminopropyltriethoxysilane (KH550) was provided by Nanjing Zhongdong Chemical Glass Instrument Co., Ltd.; dimethyl sulfoxide (DMSO), potassium tert-butoxide (KTB), methanol, cyclohexane, tetraethyl orthosilicate (TEOS), and epichlorohydrin (ECH) were all provided by Sinopharm Chemical Reagent Co., Ltd.

1.2 Preparation method

Preparation of KKNFs$^@$SiO$_2$: Weigh 5g of Kevlar49 yarn and cut it into 1~2 cm segments. Soak the segments in anhydrous ethanol and subject them to ultrasonic treatment for 6 hours. After washing with deionized water and drying thoroughly, mix them with 5g of potassium tert-butoxide in a round-bottom flask containing DMSO and stir for 10 minutes. Then, add 5g of anhydrous methanol and stir for 6 hours to obtain a DMSO dispersion of KNFs. React this dispersion with 2mL of epichlorohydrin at 30°C for 24 hours to obtain modified Kevlar nanofibers (mKNFs), and wash them until neutral at 12,000 rpm. Subsequently, react them with KH550 for 5 hours, and then add 10mL of TEOS and react for 3 hours to obtain Kevlar nanofibers with in-situ grown nano-silica on the surface (mKNFs$^@$SiO$_2$). Disperse the mKNFs$^@$SiO$_2$aqueous dispersion in deionized water to obtain a dispersion with a concentration of 2.5 mg/mL. Add 0.02 mol of KH550 to the mKNFs$^@$SiO$_2$ aqueous dispersion and stir at 60°C for 2 hours to obtain KKNFs$^@$SiO$_2$. Vacuum filter the unreacted KH550 and wash it with an ethanol aqueous solution until neutral. Finally, disperse KKNFs$^@$SiO$_2$ in deionized water to obtain a dispersion with a concentration of 2.5 mg/mL and subject it to ultrasonic treatment.

Preparation of KKNFs$^@$SiO$_2$/EPDM nanocomposites: The final dispersion obtained from the previous step was stirred and dispersed with 800 mL of cyclohexane at 50°C for 2 hours to form a stable dispersion. Then, 100 g of EPDM was cut into small pieces and gradually added to the aqueous solution of KKNFs$^@$SiO$_2$. After mechanical stirring for 12 hours, the KKNFs$^@$SiO$_2$/EPDM mixed solution was vacuum distilled at 60°C until no more cyclohexane condensate was produced. The obtained wet KKNFs$^@$SiO$_2$/EPDM material was vacuum dried at 60°C until constant weight. The rubber was mixed on a rubber mill at room temperature, with the feeding sequence being as follows: 100 parts of EPDM, 5 parts of ZnO, 1 part of StA, 10 parts of ZB, 15 parts of BA, variable amount of mKNFs$^@$SiO$_2$ or KKNFs$^@$SiO$_2$, 4.5 parts of DCP, 1 part of TMTD, and 1.5 parts of S. The rubber compound was allowed to stand for 24 hours, and the optimal cure time was measured on a vulcanizer at 160°C. Subsequently, an appropriate amount of rubber compound was weighed and placed in a mold, and vulcanization was performed at 160℃ and 10 MPa to obtain KKNFs$^{@}$SiO$_2$/EPDM nanocomposites. The corresponding rubber compound formulation and sample numbers are shown in Table 1.

Table 1 Formula of KKNFs$^{@}$SiO$_2$/EPDM composite material

Sample	EPDM/phr	KKNFs$^{@}$SiO$_2$/phr	mKNFs$^{@}$SiO$_2$/phr
EPDM	100	0	0
5-mKNFs$^{@}$SiO$_2$/EPDM	100	0	5
1-KKNFs$^{@}$SiO$_2$/EPDM	100	1	0
3-KKNFs$^{@}$SiO$_2$/EPDM	100	3	0
5-KKNFs$^{@}$SiO$_2$/EPDM	100	5	0
7-KKNFs$^{@}$SiO$_2$/EPDM	100	7	0

1.3 Analysis and test

Infrared absorption spectroscopy was conducted using an FTIR-8400S infrared spectrometer, with a testing range spanning from 4,000 to 700 cm^{-1} and a testing step size of 4 cm^{-1}.

The thermal stability of the sample was tested using a DTG-60 differential thermal analyzer, with a heating rate of 10℃/min. The temperature range was 25~800 ℃.

The swelling behavior of vulcanized rubber was tested at room temperature using cyclohexane as the solvent. The sample was weighed before soaking to obtain ma. After soaking, the soaked sample, which was in swelling equilibrium and had a stable weight, was wiped and weighed to obtain ms. The crosslinking density of the sample and the average molecular weight between crosslinks can be calculated according to the following formula:

$$v_r=\frac{m_a/\rho}{(m_s-m_a)/\rho_1+m_a/\rho} \qquad (1)$$

$$v_r=\frac{In(1-v_r)+v_r+\chi v^2_r}{v_o v_r^{1/3}} \qquad (2)$$

Where ve represents the crosslinking density of the sample; v_r denotes the swelling volume fraction of the specimen; χ stands for the Flory-Huggins interaction parameter (0.465); v_o signifies the molar volume of cyclohexane; ρ is the density of EPDM before swelling; and ρ_1 indicates the density of cyclohexane.

Weigh 0.5 g of rubber compound sample (ω_1), wrap it with filter paper (ω_2), soak it in 300 ml of cyclohexane at room temperature, replace the solvent every 2 days, and soak for 7 days. Then take it out and dry it in vacuum until it reaches constant weight (ω_3). The calculation formula for bound rubber content (BdR) is as follows:

$$BdR(\%)=\frac{\omega_3-\omega_2-\omega_1 m_f/(m_f+m_r)}{\omega_1 m_f/(m_f+m_r)}\times 100 \qquad (3)$$

Where m$_f$ and m$_r$ represent the mass of rubber and filler in the rubber compound, respectively.

The tensile properties of the sample were tested using an electronic universal tensile machine of model CMT-4254. The test was conducted in accordance with the GB/T528-2009 standard, and the sample was a dumbbell-shaped test strip. The results were obtained as the average of five tests.

The ablation performance of EPDM-based insulators was tested on a test bench manufactured by Xi'an Zhirui Industrial System Engineering Co., Ltd. The experiments were conducted under conditions of oxygen-acetylene gas flow rates of 1512 L/h and 1116 L/h, and the actual heat flux was calculated to be 457 W/cm^2 using a calibrated water-cooled heat flux meter. The test samples used had a diameter of 30 mm and a height of 10 mm, with a distance of 10 mm between the sample surface and the nozzle tip. The high-speed oxygen-acetylene flame was positioned vertically at the center of the sample, and the ablation process lasted for 20 seconds. The main parameters for characterizing the ablation resistance of composite materials are the Mass Ablation Rate (*MAR*) and the Linear Ablation Rate (*LAR*), defined as follows:

$$MAR=(m_1-m_2)/t \qquad (4)$$

$$LAR=(d_1-d_2)/t \qquad (5)$$

Where m1 and d1 represent the initial mass and thickness of the sample before testing, m_2 and d_2 represent the mass and minimum thickness of the sample after ablation, and t represents the experimental time.

The cross-section of the carbon layer of the ablation sample was observed using a JSM-6380 scanning electron microscope.

2 Results and discussion

2.1 Characterization and performance testing of KKNFs$^{@}$SiO$_2$

Figure 1 shows the FTIR spectra of KNFs$^{@}$SiO$_2$ before and after modification with KH550. As can be seen from the figure, the unmodified mKNFs$^{@}$SiO$_2$ exhibits peaks at 3,300, 1,645, and 1,536 cm^{-1}, corresponding to the N-H stretching vibration, C=O stretching vibration, and N-H bending vibration of amide groups, respectively. In addition, the peaks at 1,508 and 1,306 cm-1 are attributed to the stretching vibration of aromatic rings and Ph-N vibration, respectively. A peak related to the asymmetric stretching vibration of Si-O-Si appears at 1,092 cm^{-1}, originating from the SiO$_2$ formed by the successful hydrolysis and condensation of TEOS. In KKNFs$^{@}$SiO$_2$, a primary amine N-H stretching vibration peak reappears near 1,590 cm^{-1}, accompanied by a strong sharp peak representing primary amines at 3,315 cm^{-1}, indicating that KH550 has been successfully grafted onto mKNFs$^{@}$SiO$_2$.

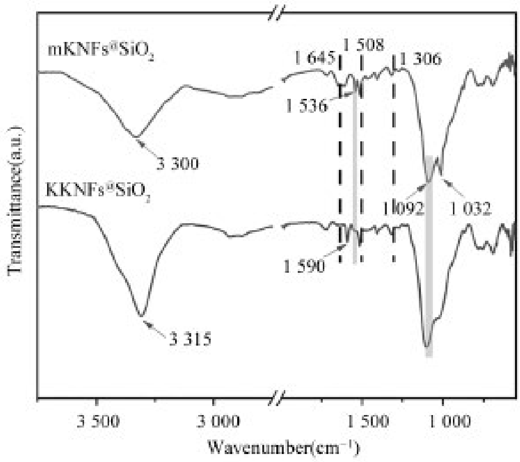

Figure 1 FTIR spectra of mKNFs$^{@}$SiO$_2$ before and after modification with KH550

Figure 2 depicts the thermogravimetric analysis of mKNFs$^{@}$SiO before and after modification with KH550. The decomposition of KKNFs$^{@}$SiO$_2$ is observed to occur in three stages. The first stage occurs below 220℃, where the weight loss of KKNFs$^{@}$SiO$_2$ is slightly higher than that of mKNFs$^{@}$SiO$_2$. This may be attributed to the further condensation and dehydration of uncondensed silanol groups in KH550 during the reaction, as well as the decomposition of a small amount of bound water adsorbed on the amino ends of KH550. The second stage occurs between 370~500℃. Compared to mKNFs$^{@}$SiO$_2$, the thermal decomposition rate is accelerated in this stage due to the introduction of more alkyl chains in KH550 (as shown in Figure 2(b)), leading to a decrease in residual weight. However, it is still significantly higher compared to unmodified KNFs. The third stage occurs between 540~700℃, primarily due to the pyrolysis of PPTA. The grafting ratio of KH550 is calculated to be 14.24% based on the formula reported in the literature. The maximum thermal decomposition temperature of KKNFs$^{@}$SiO$_2$ reaches 610.2℃, which is 3.9℃ higher than that of mKNFs$^{@}$SiO$_2$. This is due to the formation of a carbon layer during the pyrolysis of KH550 at high temperatures, which simultaneously undergoes self-condensation to generate more refractory Si-O-Si ceramic structures. These structures coat the surface of the nanofibers, hindering heat transfer and delaying the pyrolysis of KNFs at high temperatures.

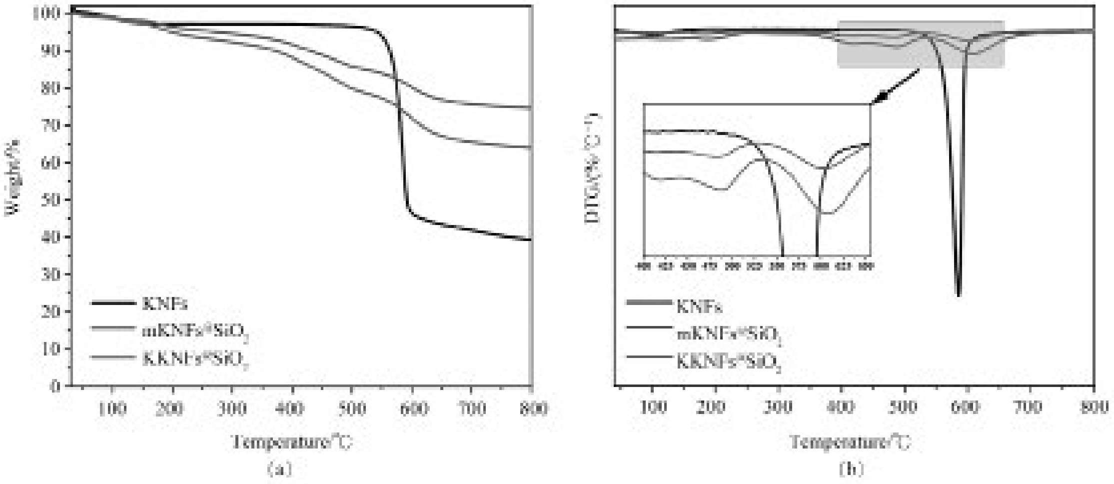

(a) (b)

Figure 2 TG(b)DTG curves of KNFs, mKNFs$^{@}$SiO$_2$, and KKNFs$^{@}$SiO$_2$

2.2 Combination of rubber and crosslinking density

Figure 3(a) shows that the BdR of EPDM is 15.63%. Compared to EPDM, the BdR of 5-mKNFs$^{@}$SiO$_2$/EPDM increased by 64.93%, and that of 5-KKNFs$^{@}$SiO$_2$/EPDM increased by 69.80%. The reinforcing effect of KKNFs$^{@}$

Table 2 Thermal decomposition data of KNFs, mKNFs$^{@}$SiO$_2$, and KKNFs$^{@}$SiO$_2$

	T_5/℃	T_{10}/℃	T_{max}/℃	R_{800}/%
KNFs	541.7	562.8	584.7	39.29
mKNFs$^{@}$SiO$_2$	275.8	430.3	606.3	74.64
KKNFs$^{@}$SiO$_2$	198.2	371.8	610.2	64.01

SiO$_2$ is more pronounced. This is due to the γ-aminopropyl groups introduced by KH550, which enhance the wetting and penetration of the nanofibers into the rubber, forming a dense and stable interpenetrating network between the nanofibers and the rubber. This creates a hybrid interfacial layer of EPDM-KH550-KNFs, thereby improving the adhesion between the rubber and KKNFs$^{@}$SiO$_2$. The increase in bound rubber content in the rubber results in KKNFs$^{@}$SiO$_2$ enhancing EPDM rubber more effectively. Figure 3(b) shows that as the content of KKNFs$^{@}$SiO$_2$ increases from 0 to 5 parts, the BdR of KKNFs$^{@}$SiO$_2$/EPDM rapidly increases. This is due to the good interfacial interaction formed by the physical crosslinking between KKNFs$^{@}$SiO$_2$ and the EPDM matrix, and the interaction continues to strengthen as the content of KKNFs@SiO2 increases. Additionally, after adding 7 parts of KKNFs@SiO2, the change in the system's BdR is relatively small, which may be due to a certain degree of agglomeration of the nanofibers in the rubber matrix.

As can be seen from Figure 3(a), the crosslinking density of EPDM is 2.01×10-4 mol/cm3. Compared to EPDM, the crosslinking density of 5-mKNFs$^{@}$SiO$_2$/EPDM is increased by 0.21%, and that of 5-KKNFs$^{@}$SiO$_2$/EPDM is increased by 61.60%. The enhancement effect of KKNFs$^{@}$SiO$_2$ is more pronounced. This is due to the difficulty in forming effective crosslinking points between mKNFs$^{@}$SiO$_2$ and EPDM. The modification with KH550 enables KKNFs$^{@}$SiO$_2$2 to disperse uniformly within the EPDM matrix, and the van der Waals interaction between it and the EPDM matrix forms new physical crosslinking points in the system, thus significantly improving the crosslinking density of the composite material. Figure 3(b) shows that the crosslinking density of EPDM is 2.20×10-4 mol/cm3. With the increase in the content of KKNFs$^{@}$SiO$_2$, the crosslinking density of 1-KKNFs$^{@}$SiO$_2$/EPDM and 3-KKNFs$^{@}$SiO$_2$/EPDM increases by 3.5% and 9.4%, respectively, which is not significant. This is because the grafted KH550 cannot react with the EPDM molecular chain to form chemical bonds, thus failing to form effective chemical crosslinking points. The crosslinking density of 5-KKNFs$^{@}$SiO$_2$/EPDM and 7-KKNFs$^{@}$SiO$_2$/EPDM increases by 61.7% and 68.1%, respectively. This is due to the prominent role of KKNFs$^{@}$SiO$_2$ as physical crosslinking points when its addition amount is high.

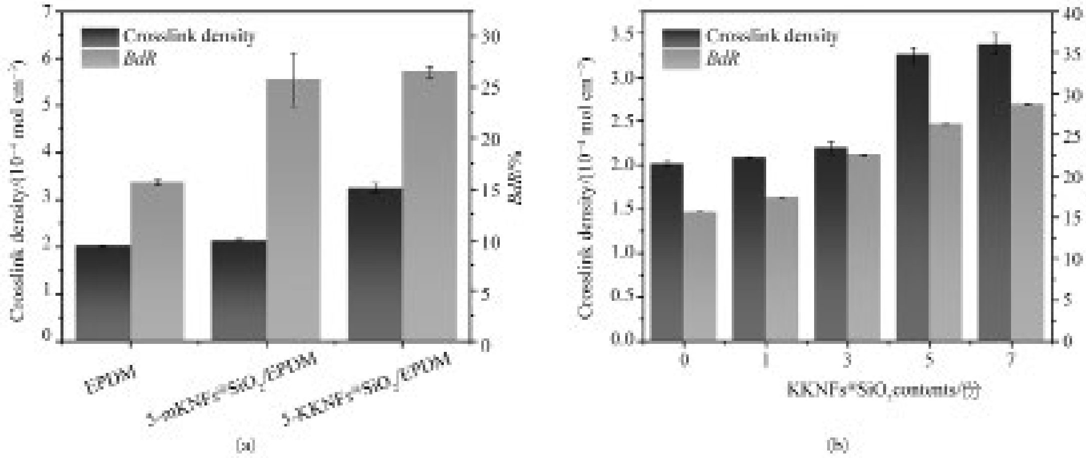

Figure 3 Combined rubber content and crosslinking density of KKNFs$^{@}$SiO$_2$/EPDM

2.3 Mechanical properties

As shown in Figure 4(a), the tensile strength and elongation at break of EPDM are 5.88 MPa and 463%, respectively. Compared to EPDM, the tensile strength and elongation at break of 5-mKNFs$^{@}$SiO$_2$/EPDM are increased by 89.4% and 30.2%, respectively. This is due to the in-situ growth of nano–SiO$_2$ on the surface of mKNFs$^{@}$SiO$_2$, which increases the specific surface area of the nanofibers.

Additionally, the surface of nano−SiO_2 contains abundant hydroxyl groups, which facilitate the adsorption and entanglement of more EPDM molecular chains, thus hindering the slippage of rubber segments under external forces and improving the tensile properties. Compared to EPDM, the tensile strength and elongation at break of 5−KKNFs@SiO_2/EPDM are increased by 235.5% and 65.4%, respectively, further enhancing the mechanical properties of the composite material. This is because, compared to mKNFs@SiO_2, KKNFs@SiO_2, grafted with KH550 containing non-polar alkyl chains, exhibits superior dispersion in the non-polar EPDM matrix.

As shown in Figure 4(b), the tensile strength of 1, 3, and 5−KKNFs@SiO_2/EPDM increased by 132.9%, 164.1%, and 228.7% respectively compared to EPDM, while the elongation at break increased by 52.7%, 72.6%, and 65.4% respectively. However, when the amount of KKNFs increased to 7 parts, the nanofibers had an adverse effect on the mechanical properties of the composite material. This is due to the agglomeration of nanofibers within the EPDM matrix caused by their nanoscale size, which prevents the smooth transfer of load when subjected to external forces, leading to stress concentration and further defects, resulting in a decrease in both tensile strength and elongation at break.

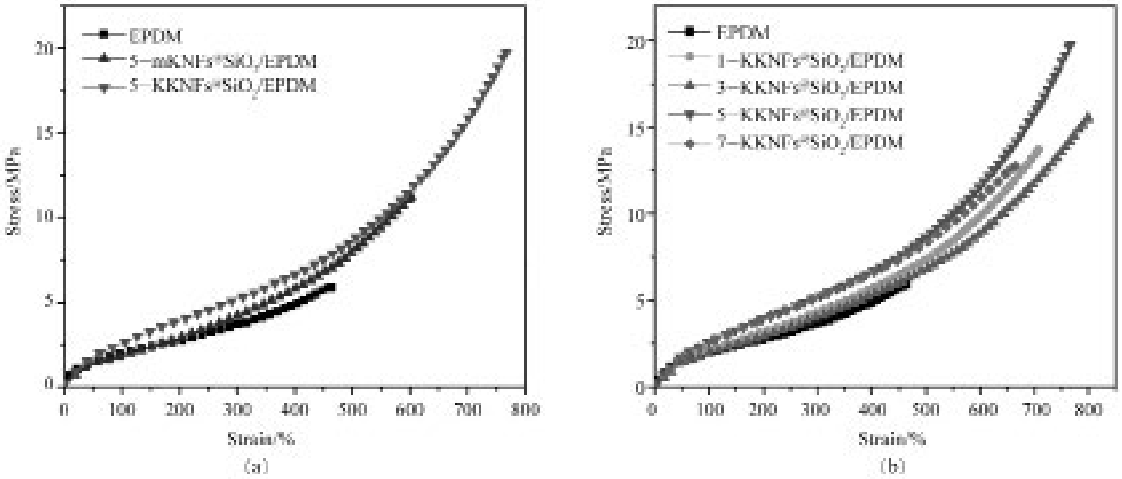

Figure 4 Stress-strain curve of KKNFs@SiO_2/EPDM composite material

Table3 Mechanical property parameters of KKNFs@SiO_2/EPDM composite materials

Sample	Tensile strength/MPa	Elongation at break, %
EPDM	5.88±0.12	463±9
5-mKNFs@SiO_2/EPDM	11.14±0.15	603±34
1-KKNFs@SiO_2/EPDM	13.70±0.67	707±31
3-KKNFs@SiO_2/EPDM	15.53±0.32	799±58
5-KKNFs@SiO_2/EPDM	19.73±0.55	766±24
7-KKNFs@SiO_2/EPDM	12.75±0.36	665±35

2.4 Thermal stability

As shown in Table 4, the temperature at 5% weight loss (T_5), temperature at 10% weight loss (T_{10}), maximum thermal decomposition rate temperature (T_{max}), and residual weight at 800 ºC (R800) of mKNFs@SiO_2/EPDM are all higher than those of pure EPDM, attributed to the thermal stability of mKNFs@SiO_2. After modification with KH550, the T_5, T_{10}, Tmax, and R800 of KKNFs@SiO_2/EPDM are further improved. This is due to the ability of KKNFs@SiO_2 to adsorb more vulcanizing agents and accelerators, promoting intermolecular crosslinking reactions, increasing the crosslinking density in the crosslinked network, restricting the movement of molecular segments, and forming a barrier to heat transfer through the nano-filler network formed by nano-SiO_2 and nanofibers, further enhancing the thermal stability of the composite material.

Table 4 shows that the R800 of EPDM is 26.75%. In comparison, the R800 of 1, 3, 5, and 7-KKNFs@SiO_2/EPDM increased by 0.52%, 5.72%, 13.08%, and 15.96%, respectively. As shown in Figure 5(b), the main weight loss stage of the KKNFs@SiO_2/EPDM nanocomposites occurs around 400-500℃. The data in Table 4 clearly indicates that as the content of KKNFs@SiO_2 increases, the Tmax of the system gradually increases. Compared to EPDM's Tmax of 453℃, the Tmax of composites with 1, 3, 5, and 7 parts of KKNFs increased to 453.3, 453.5, 454.0, and 454.2℃, respectively. The corresponding maximum thermal decomposition temperatures are shown in Figure 5(c) and Figure 5(d). This is also attributed to the excellent thermal stability of KKNFs@SiO_2 itself and the improvement in the crosslinking density of the system.

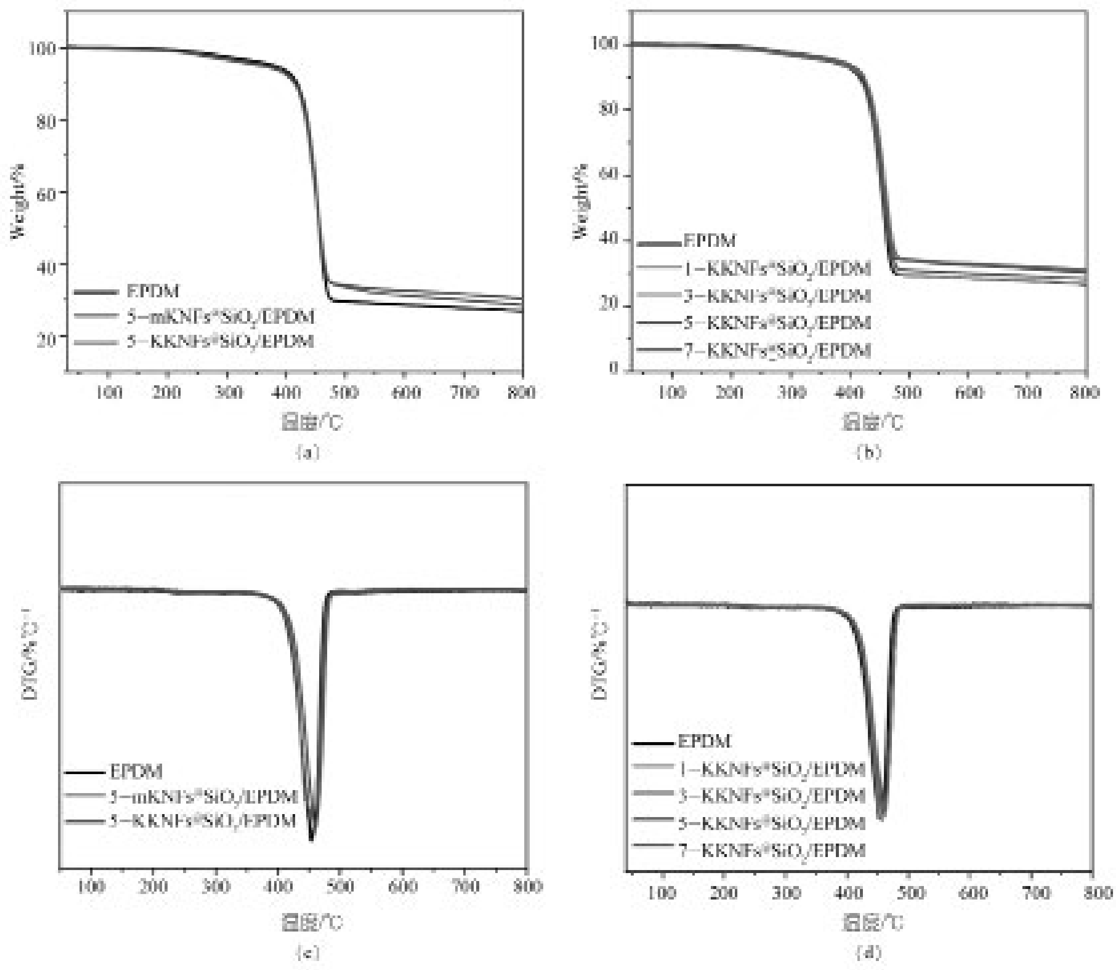

Figure 5 (a) TGA and (b) DTG curves of KKNFs$_@$$SiO_2$/EPDM nanocomposites

Table 4 Thermal decomposition data of KKNFs@SiO_2/ EPDM nanocomposites

	T_5/°C	T_{10}/°C	T_{max}/°C	R_{800}/%
EPDM	351.7	409.2	453.0	26.75
5-mKNFs@SiO_2/EPDM	358.2	413.6	453.7	28.83
1-KKNFs@SiO_2/EPDM	356.3	418.3	453.3	26.89
3-KKNFs@SiO_2/EPDM	361.6	420.0	453.5	28.28
5-KKNFs@SiO_2/EPDM	360.3	414.8	454.0	30.25
7-KKNFs@SiO_2/EPDM	383.3	422.9	454.2	31.02

2.5 Ablation performance

As shown in Figure 6(a), the LAR and MAR of EPDM are 0.253 mm/s and 0.129 g/s, respectively. In comparison, the LAR and MAR of 5-mKNFs@SiO_2/EPDM decreased by 46.64% and 34.11%, respectively. After surface grafting with KH550, the enhancement effect of KKNFs@SiO_2 on the ablation resistance of the composite material was further enhanced. The LAR and MAR of 5-KKNFs@SiO_2/EPDM decreased by 69.9% and 47.6%, respectively, compared to EPDM. On the one hand, the nano-SiO2 and KH550 coated on the surface of KKNFs@SiO_2 form a layer of Si-O-Si film that is difficult to decompose after ablation, making KKNFs@SiO_2 possess high char yield and high temperature resistance; on the other hand, the high crosslinking density of the previously demonstrated KKNFs@SiO_2/EPDM system means that a denser crosslinked structure is formed inside the system, which gives the composite material higher thermal decomposition resistance, thus achieving excellent ablation resistance. Figure 6(b) shows that as the content of KKNFs@SiO_2 increases, both the LAR and MAR of the composite material continuously decrease. The LAR and MAR of 7-KKNFs@SiO_2/EPDM are

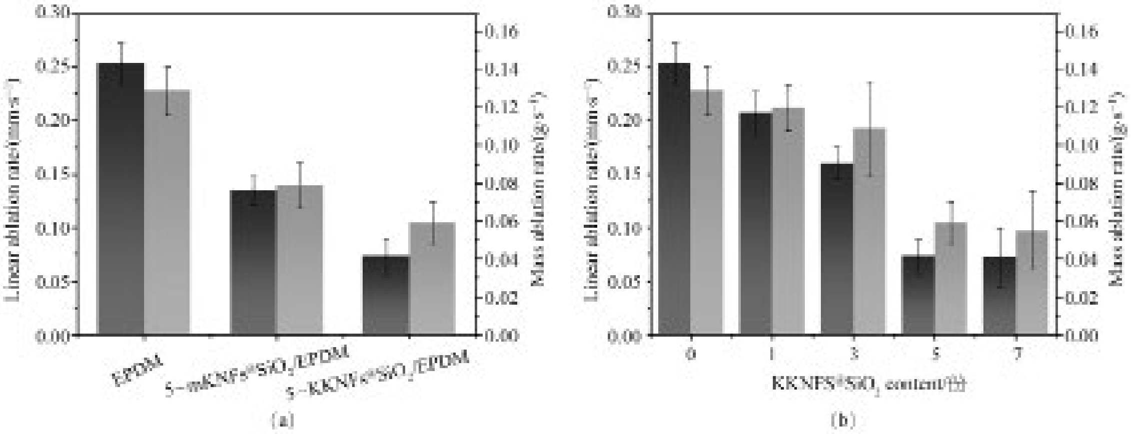

Figure 6 LAR and MAR of KKNFs$^{@}$SiO$_2$/EPDM composite material

0.072 mm/s and 0.055 g/s, respectively, which decreased by 69.9% and 39.7% compared to EPDM. This further demonstrates the significant improvement of KKNFs$^{@}$SiO$_2$ on the ablation resistance of composite materials.

2.6 Analysis of carbon layer

Figure 7 illustrates the morphological structure of the ablation surface layer of the KKNFs$^{@}$SiO$_2$/EPDM composite observed under SEM at different magnifications. As shown in Figure 7(a$_1$), the pure EPDM carbon layer exhibits a loose and porous structure, accompanied by irregular deposits on the surface. As shown in Figure 7(a$_2$), when observing the local carbon layer at a high magnification, it can be seen that the carbon layer is layered and stacked, with irregular cracks and pores, indicating that EPDM cannot form a high-strength and dense carbon layer under ablation experimental conditions. Therefore, its linear ablation rate and mass ablation rate are relatively high. Figures 7(b$_1$) and (b$_2$) depict the morphology of the ablation carbon layer of KKNFs$^{@}$SiO$_2$/EPDM. Compared to EPDM, the carbon layer of KKNFs$^{@}$SiO$_2$/EPDM is the most dense, with no obvious pores; further observation at a high magnification reveals that nano-silica has been transformed into nano-sized silicon oxide particles and a skeleton structure. During ablation, a large number of Si-O bonds on the surface of KKNFs$^{@}$SiO$_2$ are opened during pyrolysis, forming a refined cross-linked network structure and abundant SiOx after carbonization. Driven by the pyrolysis gas flow, the molten SiOx on the surface of KKNFs$^{@}$SiO$_2$ reacts with hydrocarbons to generate irregular SixOyCz spherical particles. These spherical particles have a high specific surface area, which can adhere to more residual carbon, filling the pores between the carbon layer skeletons. On the one hand, this makes the carbon layer structure denser, and on the other hand, the high thermal stability of silicon oxides themselves can also enhance the ablation resistance of the composite material.

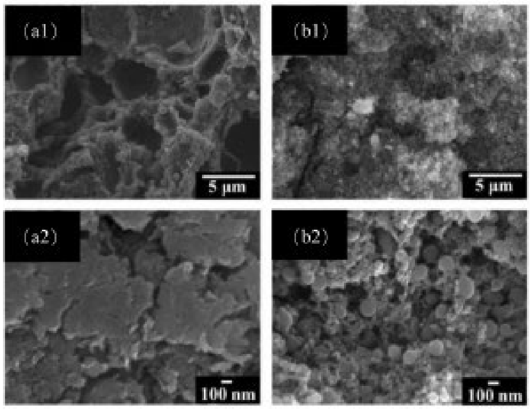

Figure 7 SEM images of the char layer on the ablated surface of EPDM (a1-2) and 5-KKNFs$^{@}$SiO$_2$/EPDM (b1-2)

3 Conclusion

(1) KH550 can significantly enhance the interaction between KNFs$^{@}$SiO$_2$ and EPDM, thereby increasing the bonding rubber and crosslinking density of EPDM.

(2) With the increase in the amount of KKNFs$^{@}$SiO$_2$/EPDM, the tensile strength and elongation at break of EPDM continue to increase. When the amount of KKNFs$^{@}$SiO$_2$ is 5 parts, the comprehensive performance of EPDM is optimal.

(3) Compared to EPDM without filled KKNFs$^{@}$SiO$_2$, the tensile strength and elongation at break of the 5-KKNFs$^{@}$SiO$_2$/EPDM nanocomposite increased by 235.5% and 65.4%, respectively, while the linear ablation rate and mass ablation rate decreased by 69.9% and 47.6%, respectively.